

Precipitation interpolation, autocorrelation, and predicting spatiotemporal variation in runoff in data sparse regions: Application to Panama

Shriram Varadarajan^{a,*}, José Fábrega^{d,e}, Brian Leung^{a,b,c}

^a Department of Biology, McGill University, Montreal, Quebec H3A 1B1, Canada

^b Bieler School of Environment, McGill University, Montreal, Quebec H3A 2A7, Canada

^c Smithsonian Tropical Research Institute, PO Box 0843-03092, Panamá City, Panamá

^d Universidad Tecnológica de Panamá, Campus Víctor Levi Sasso, Ancón, Vía Centenario, Panamá City, Panamá

^e Member of the National Research System of Panama (SNI)

ARTICLE INFO

Keywords:

Hydrological modeling
Soil and water assessment tool
Neotropical hydrology
Spatial autocorrelation

ABSTRACT

Study region: Panama faces seasonal floods and droughts, and rising freshwater demand for domestic consumption, hydropower, and the operation of the Panama Canal. A process-based hydrological model of the country would complement the existing national water security plan as a scenario planning tool.

Study focus: In Panama, as in much of the Global South, sufficient observed data do not exist for all watersheds to calibrate complex hydrological models. Understanding and improving the performance of uncalibrated hydrological models could greatly expand their utility in such regions. In this study, we build and validate an uncalibrated Soil and Water Assessment Tool (SWAT) model for Panama. We extend the default precipitation submodel and demonstrate the importance of accounting for spatial autocorrelation patterns in precipitation inputs: we found large improvements over the default model, not only for monthly means (NSE = 0.88, from 0.69 for default SWAT), but especially for standard deviations (NSE = 0.59, from 0.27) and maxima (NSE = 0.51, from 0.21) of discharge across locations and months.

New hydrological insights for region: We found a strong seasonal trend and regional differences in the spatial autocorrelation of rainfall, suggesting that this phenomenon should not be modeled statically. The resulting precipitation and hydrology models provide important baseline information for Panama, especially on variability and extremes, and could serve as a template for other regions with limited data.

1. Introduction

The potential impacts of changes in the hydrological cycle brought about by climate change and human activity range from shortages of potable water (F.A.O., 2018, p. 31) to increasing frequency and impact of floods and droughts (e.g., Hirabayashi et al., 2013). Changing patterns of precipitation and hydrology also strongly influence local vegetation and may negatively affect

* Corresponding author.

E-mail addresses: shriram.varadarajan@mail.mcgill.ca (S. Varadarajan), jose.fabrega@utp.ac.pa (J. Fábrega), brian.leung2@mcgill.ca (B. Leung).

<https://doi.org/10.1016/j.ejrh.2022.101252>

Received 16 February 2022; Received in revised form 17 October 2022; Accepted 29 October 2022

Available online 1 November 2022

2214-5818/© 2022 The Authors. Published by Elsevier B.V. This is an open access article under the CC BY-NC-ND license (<http://creativecommons.org/licenses/by-nc-nd/4.0/>).

biodiversity (e.g., distance to water and precipitation were found to be two of the best predictors of species distributions, [Bradie and Leung, 2017](#)). The capacity to predict the nature of changes in hydrological patterns will be crucial for effective risk mitigation and building systemic resilience. Given spatial heterogeneity in these dynamics, identifying critical regions at high risk for reductions in water availability and increases in extreme events must be an integral part of planning and management strategy. The need for this type of analysis is even more pronounced in the Global South, where the threat of climate change is compounded by economic and infrastructural inequality ([Roberts, 2001](#); [Chapagain et al., 2020](#)).

In Panama, our study area, a national framework for water resource management already exists in the form of the Plan Nacional de Seguridad Hídrica or National Water Security Plan ([Comité de Alto Nivel de Seguridad Hídrica, 2016](#)), but a process-based hydrological model of the country would be a useful complement for scenario modeling and risk assessment. The Soil and Water Assessment Tool (SWAT, [Arnold et al., 1998](#)) was chosen for this task due to its demonstrated utility in watershed modeling at larger scales (e.g., [Abbaspour et al., 2015](#), [Pagliero et al., 2014](#)) and its process representation of several interlocking systems such as agricultural practices and nutrient flows along with hydrology, which will allow for future integrated modeling of these other crucial spheres.

The utility of SWAT in simulating single watersheds with model parameters calibrated to local conditions, at least at the monthly timestep, is well established (e.g., [Perez-Valdivia et al., 2017](#)) and these studies comprise most of the SWAT literature ([Krysanova and White, 2015](#)). However, the calibration procedures are complex and require comprehensive and high-quality hydrological data (see [Arnold et al., 2012](#), [Abbaspour et al., 2017](#)), which are not available for many watersheds in most regions of the Global South. Advances have been made to address this, including regionalization approaches (e.g., [Choubin et al., 2019](#)) that comprise first calibrating on gauged basins where sufficient data exist, and then extrapolating calibrated parameter values to ungauged basins matched to gauged ones based on, for example, physical similarity and/or proximity. This approach yields improvements in model performance but still involves calibration at gauged locations, with all the concomitant data requirements. There may be other avenues of achieving satisfactory model performance as well. SWAT, being a process-based model built on physics, could in principle perform well uncalibrated. This has indeed been demonstrated for some contexts (e.g., annual water flow; [Srinivasan and Zhang, 2010](#)), but uncalibrated performance must be tested empirically and systematically for different study regions and different indices of interest (e.g., means, variability, and extremes in streamflow).

Improvements to model structure can be considered an avenue of improving predictive power that is separate from calibration ([Butts et al., 2004](#)); for example, an improved soil submodel for SWAT has been shown to improve streamflow and nitrate load predictions even in the absence of parameter calibration ([Qi et al., 2020](#)). It has also been shown that quality of precipitation input, specifically in terms of interpolation method, is an important driver of model performance even in calibrated SWAT models ([Tuo et al., 2016](#); [Xue et al., 2018](#)). However, to our knowledge, there has been little systematic evaluation of potential improvements to uncalibrated SWAT performance through improving precipitation input. One recent attempt to use an alternative precipitation product (CFSR, Climate Forecast System Reanalysis) for an uncalibrated model of a neotropical system found worse performance than simply using available gauge data ([Auerbach et al., 2016](#)), albeit in a region with higher density of rain gauges than Panama. Thus, we decided that improving the interpolation of existing gauge data would be a logical focus for our model of Panama.

In the present study we first built and tested the performance of an uncalibrated SWAT model of Panama using the default precipitation interpolation method of SWAT, and then proposed and tested modifications to the precipitation submodel that could improve model performance. We tried to improve the precipitation submodel structure by incorporating (i) regional differences in climatic patterns within Panama, by delineating separate regions based on available maps of climate zones, (ii) realistic spatial autocorrelation patterns of precipitation (interpolating gauge data in two steps, for occurrence and then quantity) within each region and for each day, and finally (iii) allowing for seasonal variation in the strength of this autocorrelation by fitting the distance-decay parameters for each month as well as each region. We demonstrate that it is crucial to capture these regional and spatio-temporal autocorrelation patterns in precipitation. For both default and modified SWAT models, we examine predictive power for water availability (mean monthly flow) as well as variability (standard deviation and maxima of flow) across space and time. We also examine the performance of the models within each watershed and identify characteristics of watersheds that explain the variation in this performance.

2. Methods

2.1. Study area – Panama

The National Water Security Plan of Panama predicts a rise in water insecurity as human consumption reaches 50% of freshwater availability in the country by 2050 ([Comité de Alto Nivel de Seguridad Hídrica, 2016](#)). Freshwater is also a key resource for the Panama Canal system, which requires 52 million gallons per ship transit. The Canal Authority came close to having to impose draft restrictions due to lack of water during the dry season in 2015, an El Niño year ([Anon, 2015](#)). The canal is uniquely important not only to Panama's economy with \$2.6 billion in revenue ([OECD, 2017](#)), but also as a key node in the global shipping trade. Additionally, about 45% of the country's electrical capacity is accounted for by hydropower ([ASEP, 2021](#)), making variability in flow patterns critical to predict. Along with droughts like the one in 2015, floods and associated landslides are also problems faced by the country (e.g., [Wohl and Ogden, 2013](#)). These changes are projected to have further downstream effects ranging from agricultural yield changes to the persistence of Chagas disease ([Fábrega et al., 2013](#)). Beyond human impacts, Panama is also at the center of one of the world's most biodiverse regions ([Myers et al., 2000](#)), and the rich tropical forests and aquatic ecosystems that support this diversity are heavily reliant on the health of its waterways.

While temperatures across Panama are quite even and vary primarily based on elevation, there is considerable variation in

precipitation patterns within the country both between regions and across time, due to a combination of topographic complexity and seasonal drivers of precipitation (Palka, 2005). The country is long and narrow, with the central spine of mountains forming a higher topographic barrier in the Western half of the country. The Pacific side of this central spine of mountains experiences a marked dry season from roughly December to April, while the Caribbean side has rainfall more evenly throughout the year, and in higher quantity in general (Fábrega et al., 2013). The primary seasonal driver of precipitation is the movement of the Intertropical Convergence Zone (ITCZ), and interannual variation is influenced by El Niño-Southern Oscillation (ENSO) cycles. These characteristics led to our choices to incorporate seasonality and regionality as two facets of the precipitation interpolation method (that is, fitting the parameters for the method to each region and to each season). Furthermore, the country's reliance on hydropower and susceptibility to floods are among the factors that led to our focus on variability and extreme events in streamflow in addition to mean values.

The 6 climatic regions in the model (henceforth just referred to as 'regions', see Fig. 2) were delineated with reference to the climatic regions outlined in Panama's national water plan document (Comité de Alto Nivel de Seguridad Hídrica, 2016, p. 22) as well as the latest Köppen climate classification maps (Beck et al., 2018). Both sources were consistent in separating the Caribbean & Pacific faces of the Tabasara mountains, the Azuero peninsula, and the central Canal region (regions 1, 2, 3, and 4 respectively). The part of the country to the East of the canal was grouped into a single region in the water plan document but the Köppen map shows a gradation with more tropical savannah (Köppen classification 'Aw') in the western half surrounding Lake Bayano (model region 5) and more tropical rainforest (Köppen 'Af') in the Darien (region 6).

2.2. SWAT model setup

In this study, we use SWAT to build a countrywide hydrological model of Panama. SWAT is a process-based model that incorporates information about meteorology, physical geography, and human land use to simulate the entire hydrological cycle of the study area. Spatial variation is made explicit in SWAT by splitting each watershed into 'subbasins' of non-branching stream segments and their drainage areas, and further splitting each subbasin into a set of Hydrological Response Units (HRUs) which represent a particular combination of slope, land use, land management, and soil type. SWAT can thus provide sophisticated and holistic hydrological projections for given patterns of changes in its inputs.

The SWAT model requires a set of spatially explicit inputs for the study area: a digital elevation model (DEM), a soil map, a land use map, and a set of weather station locations. The weather stations further must be provided with precipitation, solar radiation, relative humidity, and wind data in the form of either (i) records for each day of the simulation or (ii) parameters for a rainfall distribution that the model samples from on each simulated day. The data sources used for each of the above in the current study are summarized in Table 1. Data on river discharge from the ETESA (Empresa de Transmisión Eléctrica, S.A.; <https://www.etsa.com.pa/>) hydrological monitoring network from the period 2005 – 2015 was used for model validation, while ETESA precipitation data from the periods 1990 – 2000 and 2005 – 2015 were used for fitting the precipitation submodel parameters and running the validation simulation respectively. All the above rain gauges and hydrological monitoring stations are mapped in Fig. 1. The three main lakes/reservoirs of note in the study area are Lake Gatún, Lake Alajuela, and Lake Bayano. All three were modeled as reservoirs in SWAT using the.res input file and estimates of volume/area from Lewis et al. (1971) and ETESA.

Watershed delineation was carried out in ArcSWAT. A threshold of 5000 cells was chosen as the minimum inflow into an outlet for which a subbasin would be defined, which amounts to a drainage area of about 4.75 km² given the DEM cell size (1 arc-second) at the equator (~30.8 m). Areas smaller than this which drain directly into the sea or either neighboring country were not part of the model, resulting in a model delineation covering roughly 65,000 km² or 86% of the total land area of Panama. SWAT further assigns each non-branching segment of stream its own subbasin unit and calculates HRUs within each subbasin based on existing combinations of soils, land use, and slope. SWAT generates daily mean discharge output (m³s⁻¹) at the outlet of each subbasin, so additional outlets were manually defined at the location of each hydrological measurement station (52 in total) to provide direct comparison points. This

Table 1
Data sources for building the SWAT model.

Data layer	Source
DEM (Digital Elevation Model)	USGS Earth Resources Observation And Science (EROS) Center. (2017). Shuttle Radar Topography Mission (SRTM) 1 Arc-Second Global [Data set]. U.S. Geological Survey. https://doi.org/10.5066/F7PR7TFT
Soil map	FAO-UNESCO Soil Map of the World, accessible at https://data.apps.fao.org/map/catalog/srv/eng/catalog.search#/metadata/446ed430-8383-11db-b9b2-000d939bc5d8
Land use map	i. For fitting the precipitation submodel, simulation period 1990 – 2000; Land cover product using AVHRR (Advanced Very High Resolution Radiometer) data from 1992 to 1993. Hansen et al. (2000). ii. For the validation simulation, 2005 – 2015; "Panama 2012 Forest Cover and Land Use", STRI GIS Data Portal, accessible at https://stridata-si.opendata.arcgis.com/maps/SI::panama-2012-forest-cover-and-land-use-tile-layer/about
Precipitation & discharge	ETESA hydrological and meteorological stations (https://www.hidromet.com.pa/es/), STRI meteorological stations
Other climate variables (Solar radiation, wind, relative humidity, temperature)	National Centers for Environmental Prediction (NCEP) Climate Forecast System Reanalysis (CFSR) data, available at https://globalweather.tamu.edu/
Reservoir information	ETESA, Lewis et al. (1971)
Climatic regions	Comité de Alto Nivel de Seguridad Hídrica (2016), Beck et al. (2018)

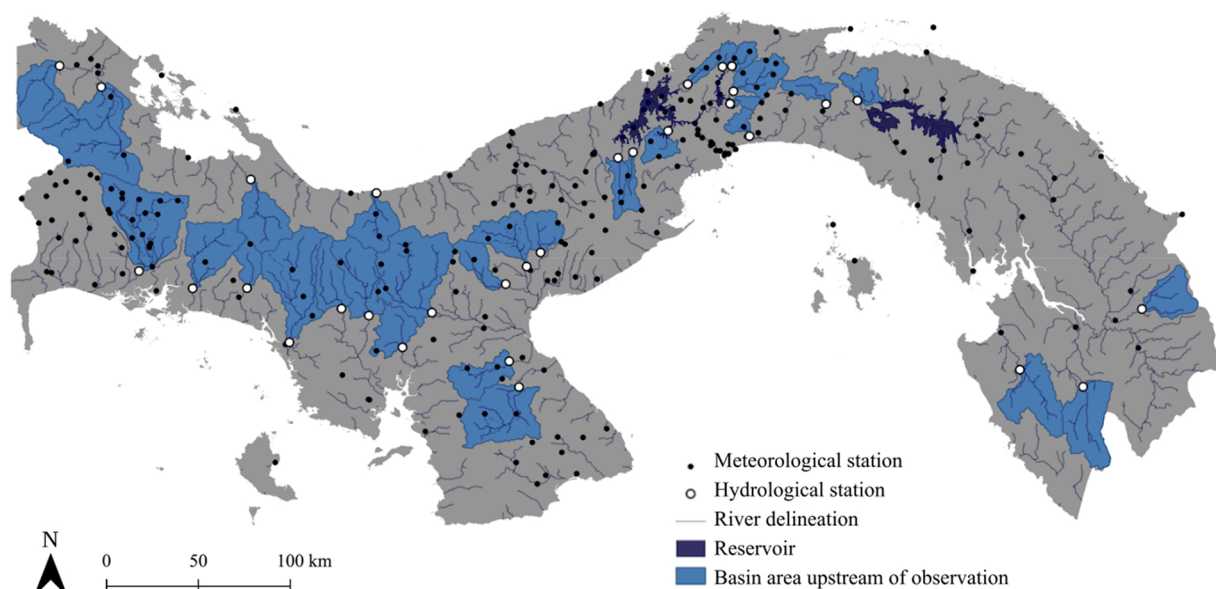


Fig. 1. Map of meteorological and hydrological stations used in simulation. Basin area upstream of gauge locations used for validation highlighted in blue (30 basins), all other regions were ungauged for the period of 2005 – 2015. Not all meteorological stations are necessarily active at any given point.

resulted in a delineation of 980 subbasins in total.

2.3. Precipitation interpolation

Daily precipitation data from ETESA was downloaded for 249 rain gauge locations across Panama, of which 120 were active during the simulation period of 2005–2015, though many had substantial temporal gaps in their records. SWAT requires daily precipitation values for each subbasin (980 in total in the current model) and thus some method of interpolation is required to fill both spatial and temporal gaps in the data coverage. For spatial gaps, the method used by default is a nearest neighbor (or Thiessen polygon) interpolation from each subbasin centroid to the nearest rain gauge. For temporal gaps, the default method is sampling from an empirically determined rainfall distribution at rain gauge locations using a skew-normal distribution (see [Neitsch et al., 2011](#)). Means, standard

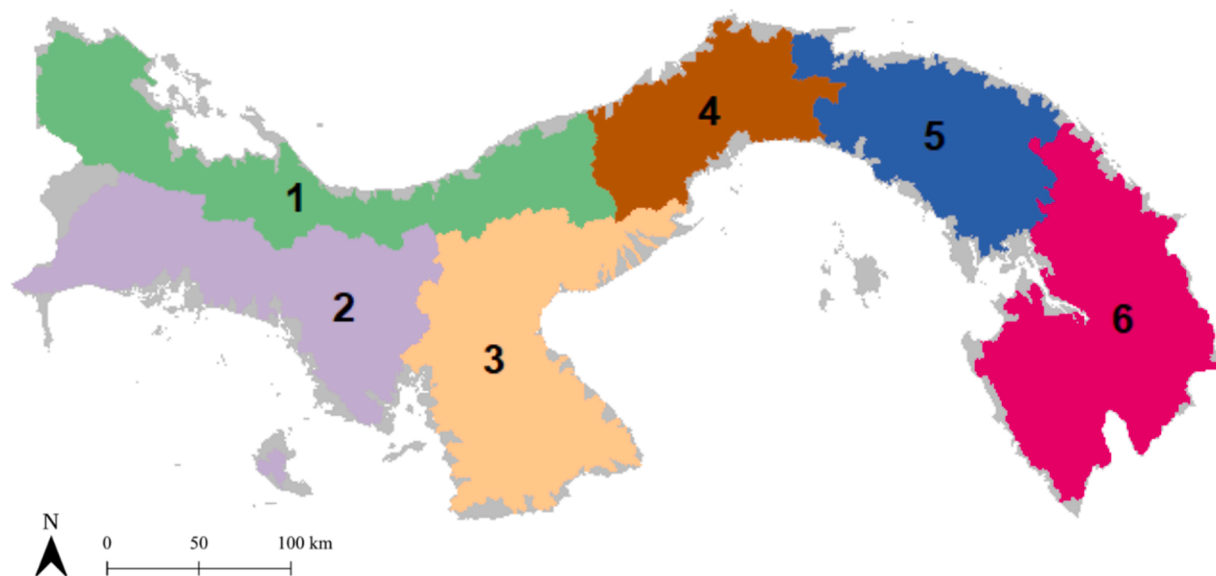


Fig. 2. Climatic regions as delineated on the area covered by the SWAT model. 1 – Caribbean side of the Tabasará mountains, 2 – Pacific side of the Tabasará mountains, 3 – Azuero peninsula, 4 – Central Panama, 5 – East-Central Panama, 6 – Darien region.

deviations, skew, and wet-dry transition probability values were calculated at all gauge locations using the observations spanning the period of 1990–2000. Henceforth this method will be referred to as the default model. This spatial interpolation method can result in locations sampling from gauges that are in different climatic zones (e.g., across the peaks of a mountain range), while the temporal interpolation method results in breaking of spatial autocorrelation patterns due to independent sampling at spatially related locations, which tends to drive overall flow down towards the mean, reducing variance and the magnitude of extremes in streamflow. Instead, we expect precipitation patterns to be spatially autocorrelated, but that the strength of autocorrelation may change seasonally with climatic forcing. We also expect regional gauge data to be more informative than just the nearest neighbor, at least for some regions and months.

In our modified method, interpolation of precipitation gauge data at each subbasin centroid was carried out for each day, and separately for each of six climatic regions that the country was split into (Fig. 2). We first tested a single-step inverse-distance weighting model, with a single distance-decay parameter (α , see Eq. 1) fit by region and month (this model was named 'RDW1', for 'single-step regional distance weighting'). Then, we tested a two-step method ('RDW2') at each location which incorporated an explicit prediction of rainfall occurrence: (1) first we predicted the probability of a wet or dry day (occurrence) using a logistic regression on the inverse distance-weighted mean of observations in the region (using a threshold observation < 0.5 mm, dry gauges were given a value of 0 and wet gauges a value of 1); (2) then, given the probability of a wet day, we performed a binomial trial; and if a wet day was generated, we interpolated the quantity of rain, again using an inverse distance weighted mean of all observed quantities of precipitation within the region for that day. Dry days were assigned a quantity of 0 mm. The two steps involved a single parameter each, α_1 and α_2 , which controlled the decay of the relative weighting with distance. Eq. 1 represents the interpolation process we used, where p_{ikt} was the precipitation value of interest (i.e., either a predictor of wet/dry through a logistic regression, or the quantity of rain in mm) for month t and region k , p_{jkt} denoted all measured precipitation values, d_{ijkt} was the distance between points i and j , and α_{kt} was a shape parameter.

$$p_{ikt} = \frac{\sum_j p_{jkt} e^{-\alpha_{kt} d_{ijkt}}}{\sum_j e^{-\alpha_{kt} d_{ijkt}}} \quad (1)$$

These α_{kt} values were fit separately to each monthly time interval and each of 6 regions in Panama, to capture expected differences in spatial and seasonal autocorrelation patterns. In the RDW2 model, the predicted total quantity of rain across a region on a given day (q_1) was reallocated to those locations that were predicted to be wet on that day (with a total quantity q_2 , where $q_2 \leq q_1$), i.e., the predicted quantity in each of these locations was scaled by the ratio q_1/q_2 , to prevent underestimation caused by the independent prediction of occurrence using binomial trials.

Each fitted parameter (α in Eq. 1) represented the strength of the distance-weighting, with high α severely penalizing information from gauges further away from the target point and prioritizing immediate neighbors. The fitting process, minimizing the sum of squared deviations, was run using the gauge data from 1990 to 2000, and the fitted algorithm was then used to interpolate daily values at the 980 subbasin centroids using gauge data from 2005 to 2015 for the validation run.

2.4. Model evaluation

As the objective was to gain insight into patterns of water distribution, the hydrological model results were compared against river discharge data from ETESA, which was not used to calibrate or parameterize any part of the models. R^2 , Nash-Sutcliffe Efficiency (NSE, Nash and Sutcliffe, 1970), and percentage bias ('Pbias') of mean model predictions against mean observed daily discharge values were calculated for each calendar month and station across the entire simulation period and these were used as metrics of the ability to predict average flow.

We also used NSE, R^2 , and Pbias to examine the ability of the hydrological model to estimate variation in runoff at a given location, using as metrics (i) standard deviation of discharge and (ii) the magnitudes of the 3 highest daily discharge events across the simulation period in each location-month combination. We chose the latter to represent of the extreme highs of the discharge distribution for that combination and as a coarse indicator of flood risk.

Finally, we used NSE and R^2 to examine the model's ability to simulate the observed monthly time series of mean discharge within each basin from 2005 to 2015. Instead of spatial variation across locations, this procedure tested the ability of the model to capture temporal variation within each watershed (using the lowermost hydrological station in each of 35 watersheds). We posited several variables across that could explain variation in model predictiveness, namely: (i) elevation of the observation (as we did not account for orographic effects explicitly), (ii) existence of a precipitation gauge within the same subbasin as the observation and (iii) number of precipitation gauges in the region (both as measures of the relevance and quantity of precipitation information), (v) number of subbasins in the watershed (as larger watersheds could have more complex behaviour), (vi) number of subbasins downstream from the observation (as interior reaches could behave differently regardless of elevation), and (vi) simulated standard deviation of mean monthly discharge at the location (as the ability to predict flow might depend on variability). We used a stepwise forward selection algorithm in R to arrive at the linear combination of these variables and their pairwise combinations with the lowest AIC value.

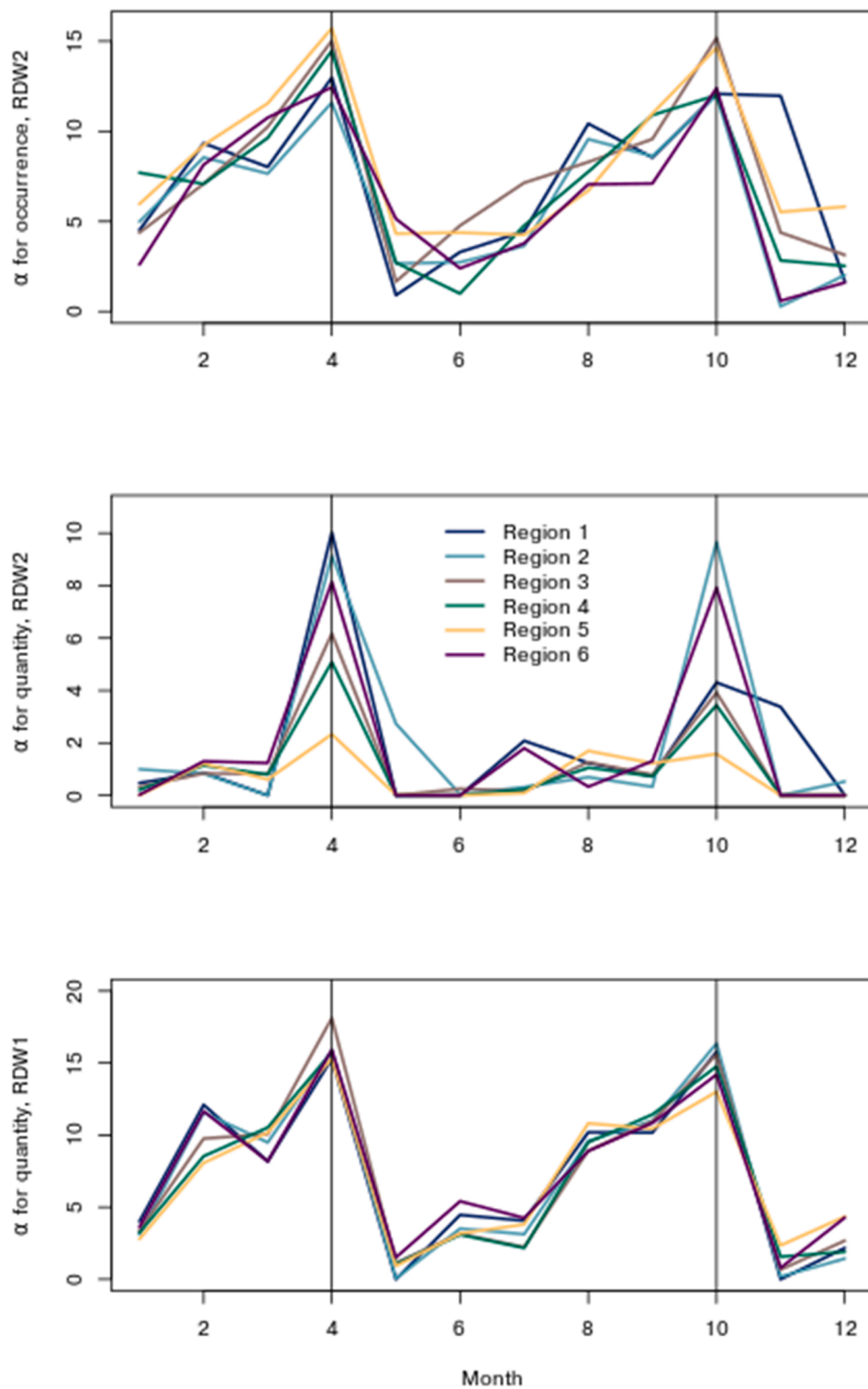


Fig. 3. Distance weighting parameter values for RDW1 (α_0) and RDW2 (α_1 for occurrence, α_2 for quantity) models. A higher value of the parameter indicates that closer neighbours are weighted much higher than ones further away, and a lower value indicates a slower distance-decay function and thus a more even distribution of weights across the region.

3. Results

3.1. Precipitation interpolation

In the regional distance weighted (RDW1 and RDW2) models, there was a strong seasonal signal in the autocorrelation patterns as represented by the fitted distance-decay parameters (α , Fig. 3). Maximum values of the α parameters correspond to the greatest weighting of the closest stations and, correspondingly, the fastest decay in weighting with distance. These maxima consistently occurred for both precipitation occurrence and quantity in April and October, and these months represent the two transitions between the wet (generally May to November) and dry seasons. Over the remainder of each season, parameter values decline and then rise gradually (for both the single parameter in RDW1 and the occurrence parameter in RDW2) or remain generally low (for the quantity parameter in RDW2) until the next seasonal transition. Variation across region was comparatively higher for both RDW2 parameters than for the single RDW1 parameter.

3.2. Model evaluation

The standard SWAT model using default precipitation interpolation performed reasonably well for mean discharge across locations with an NSE of 0.69. Improving the precipitation interpolation approach yielded even better predictions; NSE = 0.88 using the RDW2 model and NSE = 0.89 using the RDW1 model. While the default model worked well for mean discharge (NSE = 0.69), it was less able to capture variability, with NSE = 0.26 for standard deviation of locations-month combinations. In contrast, for standard deviation, the RDW2 model achieved NSE = 0.59 and RDW1 NSE = 0.53, which compared very favorably with the default model. For predicting maxima of daily discharge at each location-month combination, we found again that the default model performed poorly, with NSE = 0.22, while the RDW2 model achieved a higher NSE of 0.53, and RDW1 again performed similarly to RDW2 with NSE = 0.51. Notably, however, Pbias values were significantly larger in magnitude for the RDW1 model than for RDW2 across all analyses. These results are summarized in Table 2 and Fig. 4.

We also examined the ability to predict temporal patterns within each watershed for the default and RDW models across the ten-year period (Fig. 5). We found that the default model performed generally poorly, being a worse predictor in 24 out of 35 sites than simply using the observed mean (i.e., NSE < 0). The RDW2 model performed significantly better: while 8 sites still performed poorly (NSE < 0), 15 (43%) sites had satisfactory performance at NSE > 0.5, and the median NSE was 0.4 across locations. The RDW1 model performed intermediately, with no sites achieving NSE > 0.5 and a median NSE of 0.21. RDW2 was chosen as the overall best model due to this as well as the lower magnitude of bias mentioned above.

While there were areas of failure, the performance of RDW2 was largely predictable. 71% of the variation in NSE across locations was explained by six variables and two interaction terms. The variables were (i) elevation, (ii) total number of rain gauges in region, (iii) number of downstream subbasins, (iv) size of watershed (i.e., number of subbasins), (v) simulated standard deviation of discharge, and (vi) presence of (of which (ii), (iv), and (vi) were significant), and the significant interaction terms were between watershed size and number of downstream subbasins, and between watershed size and simulated standard deviation (Table 3).

4. Discussion

Panama faces a variety of issues related to potential changes in the water cycle ranging from shortages of drinking water and hydropower to increased impact of floods and droughts. While sophisticated hydrological modeling tools such as SWAT exist, the data available with which to build and calibrate such models is generally more limited in Panama and other countries of the Global South. Thus, while Srinivasan and Zhang (2010) demonstrated that an uncalibrated SWAT model predicted streamflow similarly to calibrated ones in the Upper Mississippi basin of the USA, testing the performance of such a model in Panama is necessary, given differences in environmental conditions and limitations of the available input data. Indeed, we found that while the default SWAT model performed well for predicting monthly mean flow across watersheds, it fared poorly for predicting monthly standard deviations and maxima. Substantial improvements were obtained across all three metrics by using a 2-stage regional distance-weighted interpolation algorithm for precipitation (i.e., our RDW2 model).

These findings highlight the importance of validating model performance in different regions, but also the potential promise of uncalibrated models even in locations where hydrological data are limited. Standard deviations and maxima, which the default model predict poorly, represent information about streamflow distributions that are crucially important in the predictive modeling of flood

Table 2

Summary of simulation results; all statistics calculated by location and calendar month across the whole country.

Model	Summary statistics (monthly discharge, m ³ /s)								
	Mean			Standard deviation			Maxima		
	R ²	NSE	pbias	R ²	NSE	pbias	R ²	NSE	pbias
Default	0.70	0.69	-11.4	0.34	0.27	0.3	0.32	0.21	1.0
1-step regional distance-weighted (RDW1)	0.90	0.89	-15.3	0.60	0.53	-30.1	0.52	0.49	-23.5
2-step regional distance-weighted (RDW2)	0.88	0.88	-9.5	0.61	0.59	-0.9	0.53	0.51	-4.1

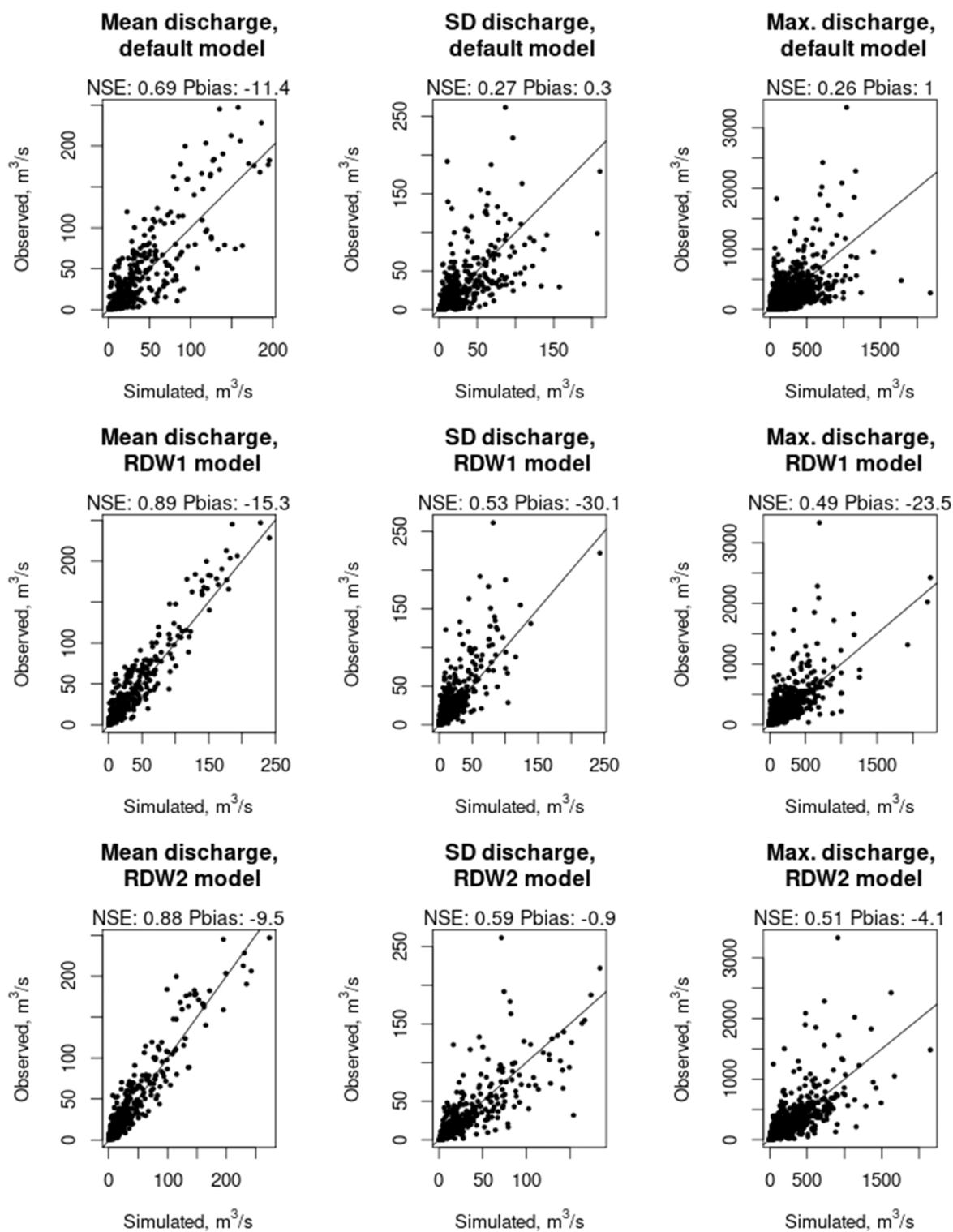


Fig. 4. Scatterplots of model performance in predicting mean monthly discharge, standard deviations, and daily maxima of monthly discharge across locations and calendar months. Each point represents a combination of a calendar month and a specific hydrological station, and all statistics are calculated over the entire simulation period (2005 – 2015).

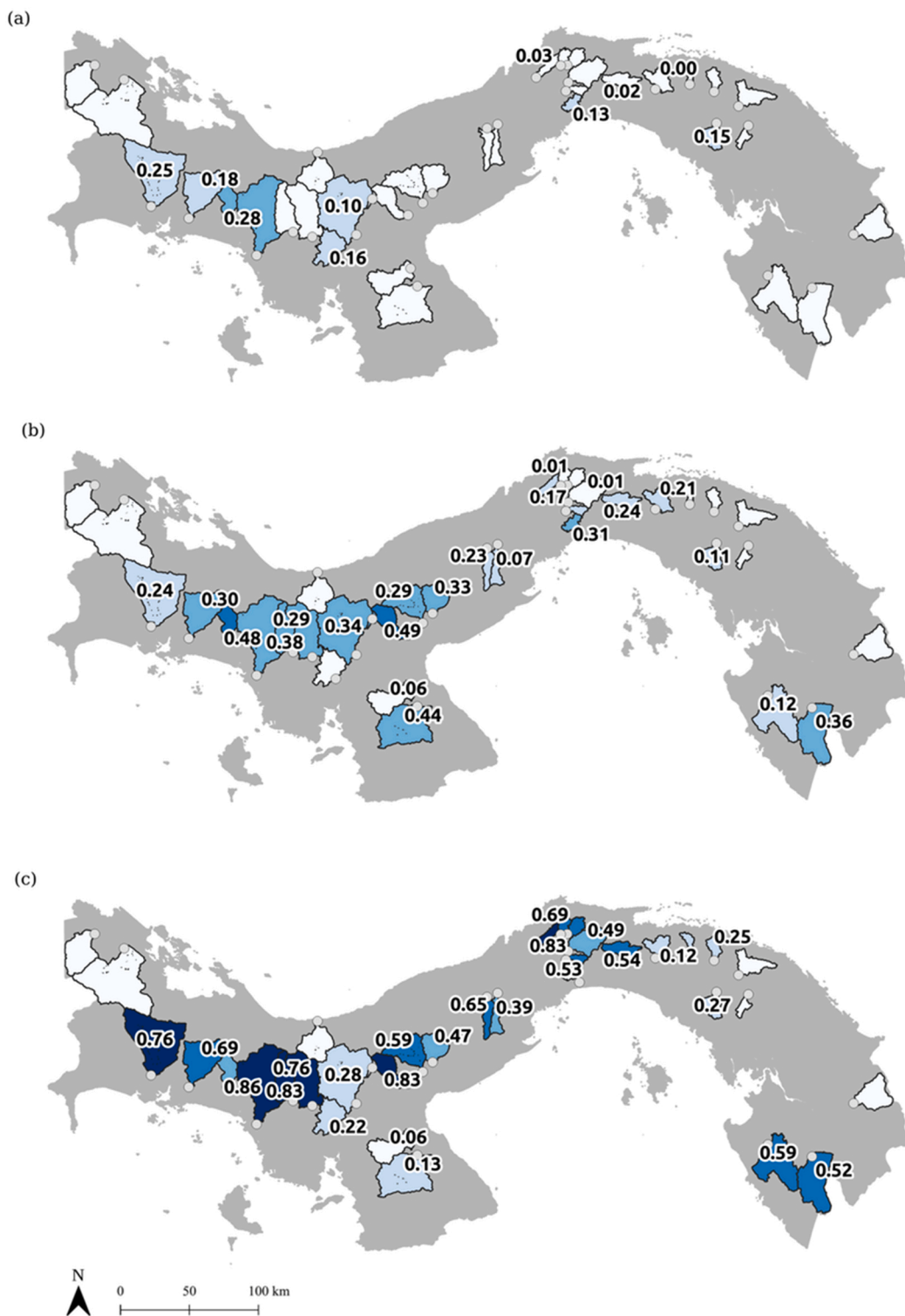


Fig. 5. NSE for prediction of mean discharge timeseries (2005 – 2015) at the monthly timestep at each basin for (a) default model, (b) RDW1 model, and (c) RDW2 model. Basins with $\text{NSE} \leq 0$ are not labeled.

risk (e.g., [van der Wiel et al., 2019](#)). Furthermore, variability in water availability is a critical indicator of potential water scarcity, and has significant impacts on human water use, despite often being overlooked in favour of annual means ([Damkjaer and Taylor, 2017](#)). Modeling studies also show that hydropower output is sensitive to variability in hydroclimatic inputs ([Arriagada et al., 2019](#);

Table 3Linear regression model summary for predictors of within-basin NSE value. AIC = 5.74, adjusted R^2 of prediction = 0.71.

Predictor	Coefficient	Std. Error	Significance (p < 0.05)
Intercept	0.55	0.07	*
1. Elevation	-0.17	0.09	
2. Total number of gauges in region	0.12	0.05	*
3. Number of downstream subbasins	0.24	0.13	
4. Size of watershed (# subbasins)	-0.28	0.08	*
5. Simulated standard deviation of discharge	-0.05	0.06	
6. Presence of rain gauge within subbasin	0.12	0.05	*
Interaction term 3 * 4	-0.38	0.09	*
Interaction term 4 * 5	-0.39	0.11	*
Interaction term 1 * 3	-0.26	0.17	
Interaction term 2 * 5	0.11	0.09	

Chowdhury et al., 2020). While future hydroclimate projections for Panama have been made for monthly mean discharge (Fábrega et al., 2013), the present study lays the groundwork for improved projections based on a more sophisticated hydrological model with higher spatial resolution and finer prediction of variability and extremes.

The relative predictive failure of the default model was due to the precipitation model which by default matches each subbasin to its nearest precipitation gauge and fills temporal gaps in the daily records of each gauge by sampling from an empirical distribution that models the behavior of that gauge (Neitsch et al., 2011). This sampling is done independently of any other gauge value on that day. As these temporal gaps occurred frequently (the mean precipitation gauge was only active on 60% of days from 2005 to 2015), the result of this independent sampling would tend to average out variability across subbasins and contribute to the observed pattern of underestimated variances and extremes of streamflow in the default model. Such spatial and especially temporal gaps in rainfall data have been shown to have significant negative impacts on SWAT performance (Tan and Yang, 2020). In contrast, due to the use of distance-weighted interpolation fitted on seasonal and regional spatial patterns of precipitation, estimated values across gauges within a region on a given day more faithfully replicated real precipitation patterns in the RDW1 and RDW2 models.

While both distance-weighted models were clear improvements on the default model, RDW2 outperformed RDW1 in terms of predicting standard deviations and maxima of discharge (in terms of both NSE and percentage bias) and also performed much better than RDW1 in predicting time series of discharge at each location (Fig. 5). Most often, distance-weighted interpolation for precipitation has been modeled as a single step calculating quantity of rain (e.g., Chen and Liu, 2012; Cheng et al., 2017; Tuo et al., 2016; Xue et al., 2018), as in the RDW1 model. Yet, two-step interpolation treating (i) the occurrence of precipitation and (ii) the quantity separately has been found to regenerate more realistic patterns of spatial variability for daily precipitation (Hwang et al., 2012), as these two factors need not be linearly related and cannot be captured with a single distance function. RDW2 is thus, overall, the best model of the three tested. Only one station with hydrological data used for validation was downstream of reservoir outflow (specifically of Lake Bayano, ETESA station ID 148–08–01), and the final model achieved a within-basin NSE of 0.21 at that station, an improvement on the default model which had $NSE < 0.01$. More precise specification and treatment of these large bodies of water is one of the key next steps to be addressed in future, as they are locally important for (among many other reasons) their direct connection to the Canal.

Better accounting for spatial relatedness of precipitation gauges was also crucial for estimating fluctuations in streamflow across time within each watershed (as opposed to variation across watersheds discussed above). The uncalibrated default SWAT model generally performed no better than simply using the mean flow in most watersheds (median $NSE < 0$), again highlighting the importance of testing in different regions and for different metrics. With our RDW2 model, the median watershed NSE was 0.4% and 43% of locations achieved $NSE > 0.5$, defined to be ‘satisfactory’ performance by Moriasi et al. (2007). Furthermore, we could largely identify where failures in the RDW2 model occurred, explaining 71% of the variation in basin NSEs, and showed that the total number of gauges in the region and the presence of a gauge in the subbasin itself were both predictors of higher NSE at a given location.

Additionally, our findings suggest that spatial patterning of rainfall varied over time, with peaks in parameter values of the distance-weighted interpolation kernel in the months of April and October. High parameter values indicate that nearby gauges are much more predictive of precipitation at a point than ones further away. Low parameter values on the other hand indicate a broader averaging, and more regional forcing. The two months of highest parameter values, April and October, coincide with the periods of change in patterns of observed variation in rainfall (Fábrega et al., 2013) as well as periods of strongest increase and decrease in average rainfall respectively (Kusunoki et al., 2019). Further elucidation of the processes that lead to the variation in spatial autocorrelation captured by the current model may aid in the development of a dynamical procedure that can account for nonstationarity. While seasonal and regional patterns of spatial autocorrelation in precipitation and their effects on extreme events are being studied in some arid and semi-arid areas in regions such as China (Xu et al., 2021) and Iran (Darand et al., 2017; Rousta et al., 2017), they remain understudied in the tropics where they may also be of importance.

5. Conclusions

The main finding is that the default precipitation model of SWAT was a key limitation in applying it to Panama, and that modifying it to account for regional and seasonal patterns of spatial autocorrelation of precipitation dramatically improved predictions of flow across a range of metrics.

While the treatment of precipitation input remains a key element, further improvement of the model could incorporate integration with a regionalization approach to improve the accuracy of physical SWAT parameters or focusing on parameterizing areas of interest using direct field measurements. We focused on the streamflow output, one of the most fundamental hydrological variables, but SWAT also has the capacity for integrative modeling of other aspects of the hydrological system such as sediment load and nutrient pollution in runoff, and these represent natural avenues for future work. Finally, more precise treatment of reservoirs and the Canal system in general is an important next step.

Our model demonstrates that careful treatment of spatial autocorrelation in precipitation input can yield substantial benefits for prediction, even in regions where data limitations make hydrological calibration difficult.

Funding

NSERC (National Science and Engineering Research Council of Canada) Discovery Grant to Brian Leung. MSSSI (McGill Sustainability Systems Initiative) grant to Brian Leung.

CRediT authorship contribution statement

Shriram Varadarajan: Conceptualization, Methodology, Software, Validation, Formal analysis, Investigation, Writing – original draft, Writing – review & editing, Visualization, Data curation, **José Fabrega:** Conceptualization, Methodology, Investigation, **Brian Leung:** Conceptualization, Methodology, Formal Analysis, Writing – original draft, Writing – review & editing, Funding acquisition, Supervision.

Declaration of Competing Interest

The authors declare that they have no known competing financial interests or personal relationships that could have appeared to influence the work reported in this paper.

Data Availability

All data of simulation results and code used in the present analysis are available at <https://doi.org/10.5281/zenodo.6111112>.

References

- Abbaspour, K.C., Vaghefi, S.A., Srinivasan, R., 2017. A guideline for successful calibration and uncertainty analysis for soil and water assessment: a review of papers from the 2016 international SWAT conference. *Water* 10, 6. <https://doi.org/10.3390/w10010006>.
- Abbaspour, K.C., Rouholahnejad, E., Vaghefi, S., Srinivasan, R., Yang, H., Kløve, B., 2015. A continental-scale hydrology and water quality model for Europe: calibration and uncertainty of a high-resolution large-scale SWAT model. *J. Hydrol.* 524, 733–752. <https://doi.org/10.1016/j.jhydrol.2015.03.027>.
- Arnold, D.N., Moriasi, G., Gassman, P.W., Abbaspour, K.C., White, M.J., Srinivasan, R., Santhi, C., Harmel, R.D., van Griensven, A., Van Liew, M.W., Kannan, N., Jha, M. K., 2012. SWAT: model use, calibration, and validation. *Trans. ASABE* 55, 1491–1508. <https://doi.org/10.13031/2013.42256>.
- Arnold, J.G., Srinivasan, R., Mutiah, R.S., Williams, J.R., 1998. Large area hydrologic modeling and assessment part I: model development 1. *JAWRA J. Am. Water Resour. Assoc.* 34 (1), 73–89.
- Arriagada, P., Dieppois, B., Sidibe, M., Link, O., 2019. Impacts of climate change and climate variability on hydropower potential in data-scarce regions subjected to multi-decadal variability. *Energies* 12, 2747. <https://doi.org/10.3390/en12142747>.
- Auerbach, D.A., Easton, Z.M., Walter, M.T., Flecker, A.S., Fuka, D.R., 2016. Evaluating weather observations and the climate forecast system reanalysis as inputs for hydrologic modelling in the tropics. *Hydrol. Process.* 30, 3466–3477. <https://doi.org/10.1002/hyp.10860>.
- Autoridad de Servicios Públicos (ASEP). 2021. Available from: (https://www.asep.gob.pa/wp-content/uploads/electricidad/estadisticas/2020/segundo_semestre/oferta.pdf). Accessed 15 Feb 2022.
- Autoridad del Canal de Panamá (ACP), 2015. Canal de Panamá suspende restricción al calado de buques – Canal de Panamá. URL (<https://micanaldepanama.com/canal-de-panama-suspende-restriccion-al-calado-de-buques/>) (Accessed 7.8.21).
- Beck, H.E., Zimmermann, N.E., McVicar, T.R., Vergopolan, N., Berg, A., Wood, E.F., 2018. Present and future Köppen-Geiger climate classification maps at 1-km resolution. *Sci. Data* 5, 180214. <https://doi.org/10.1038/sdata.2018.214>.
- Bradie, J., Leung, B., 2017. A quantitative synthesis of the importance of variables used in MaxEnt species distribution models. *J. Biogeogr.* 44, 1344–1361. <https://doi.org/10.1111/jbi.12894>.
- Butts, M.B., Payne, J.T., Kristensen, M., Madsen, H., 2004. An evaluation of the impact of model structure on hydrological modelling uncertainty for streamflow simulation. *J. Hydrol., Distrib. Model Intercomp. Proj. DMIP* 298, 242–266. <https://doi.org/10.1016/j.jhydrol.2004.03.042>.
- Chapagain, D., Baarsch, F., Schaeffer, M., D'haen, S., 2020. Climate change adaptation costs in developing countries: insights from existing estimates. *Clim. Dev.* 12, 934–942. <https://doi.org/10.1080/17565529.2020.1711698>.
- Chen, F.-W., Liu, C.-W., 2012. Estimation of the spatial rainfall distribution using inverse distance weighting (IDW) in the middle of Taiwan. *Paddy Water Environ.* 10, 209–222. <https://doi.org/10.1007/s10333-012-0319-1>.
- Cheng, M., Wang, Y., Engel, B., Zhang, W., Peng, H., Chen, X., Xia, H., 2017. Performance assessment of spatial interpolation of precipitation for hydrological process simulation in the Three Gorges Basin. *Water* 9, 838. <https://doi.org/10.3390/w9110838>.
- Choubin, B., Solaimani, K., Rezanezhad, F., Habibnejad Roshan, M., Malekian, A., Shamshirband, S., 2019. Streamflow regionalization using a similarity approach in ungauged basins: application of the geo-environmental signatures in the Karkheh River Basin, Iran. *CATENA* 182, 104128. <https://doi.org/10.1016/j.catena.2019.104128>.
- Chowdhury, A.F.M.K., Dang, T.D., Bagchi, A., Galelli, S., 2020. Expected benefits of Laos' hydropower development curbed by hydroclimatic variability and limited transmission capacity: opportunities to reform. *J. Water Resour. Plan. Manag.* 146, 05020019. [https://doi.org/10.1061/\(ASCE\)WR.1943-5452.0001279](https://doi.org/10.1061/(ASCE)WR.1943-5452.0001279).
- Comité de Alto Nivel de Seguridad Hídrica, 2016. Plan Nacional de Seguridad Hídrica 2015–2050: Agua para Todos. Panamá, República de Panamá.
- Damkjaer, S., Taylor, R., 2017. The measurement of water scarcity: defining a meaningful indicator. *Ambio* 46, 513–531. <https://doi.org/10.1007/s13280-017-0912-z>.
- Darand, M., Dostkamyani, M., Rehmani, M.I.A., 2017. Spatial autocorrelation analysis of extreme precipitation in Iran. *Russ. Meteorol. Hydrol.* 42, 415–424. <https://doi.org/10.3103/S1068373917060073>.

- F.A.O., 2018. The future of food and agriculture – Alternative pathways to 2050.
- Fábrega, J., Nakaegawa, T., Pinzón, R., Nakayama, K., Arakawa, O., 2013. Hydroclimate projections for Panama in the late 21st Century (SOUSEI Theme-C Modeling Group). *Hydrol. Res. Lett.* 7, 23–29. <https://doi.org/10.3178/hrl.7.23>.
- Hansen, M.C., Defries, R.S., Townshend, J.R.G., Sohlberg, R., 2000. Global land cover classification at 1 km spatial resolution using a classification tree approach. *Int. J. Remote Sens.* 21, 1331–1364. <https://doi.org/10.1080/014311600210209>.
- Hirabayashi, Y., Mahendran, R., Koirala, S., Konoshima, L., Yamazaki, D., Watanabe, S., Kim, H., Kanae, S., 2013. Global flood risk under climate change. *Nat. Clim. Change* 3, 816–821. <https://doi.org/10.1038/nclimate1911>.
- Hwang, Y., Clark, M.R., Rajagopalan, B., Leavesley, G.H., 2012. Spatial interpolation schemes of daily precipitation for hydrologic modeling. *Stoch. Environ. Res. Risk Assess.* <https://doi.org/10.1007/s00477-011-0509-1>.
- Krysanova, V., White, M., 2015. Advances in water resources assessment with SWAT—an overview. *Hydrol. Sci. J.* 60, 771–783. <https://doi.org/10.1080/02626667.2015.1029482>.
- Kusunoki, S., Nakaegawa, T., Pinzón, R., Sanchez-Galan, J.E., Fábrega, J.R., 2019. Future precipitation changes over Panama projected with the atmospheric global model MRI-AGCM3.2. *Clim. Dyn.* 53, 5019–5034. <https://doi.org/10.1007/s00382-019-04842-w>.
- Lewis, D.C., Beard, L.R., United States, 1971. Systems analysis of the Panama Canal water supply, Technical paper - Hydrologic Engineering Center; no. 27. Dept. of Defense, Dept. of the Army, Corps of Engineers, Hydrologic Engineering Center, Davis, Calif.
- Moriassi, J.G., Arnold, J.G., Van Liew, M.W., Bingner, R.L., Harmel, R.D., Veith, T.L., 2007. Model evaluation guidelines for systematic quantification of accuracy in watershed simulations. *Trans. ASABE* 50, 885–900. <https://doi.org/10.13031/2013.23153>.
- Myers, N., Mittermeier, R.A., Mittermeier, C.G., da Fonseca, G.A.B., Kent, J., 2000. Biodiversity hotspots for conservation priorities. *Nature* 403, 853–858. <https://doi.org/10.1038/35002501>.
- Nash, J.E., Sutcliffe, J.V., 1970. River flow forecasting through conceptual models part I — a discussion of principles. *J. Hydrol.* 10, 282–290. [https://doi.org/10.1016/0022-1694\(70\)90255-6](https://doi.org/10.1016/0022-1694(70)90255-6).
- Neitsch, S.L., Williams, J.R., Arnold, J.G., Kiniry, J.R., 2011. Soil and water assessment tool theoretical documentation version 2009. *Tex. Water Resour. Inst., Coll. Station*.
- OECD, 2017. Multi-Dimensional Review of Panama: Volume 1: Initial Assessment, OECD Development Pathways. OECD Publishing, Paris. <https://doi.org/10.1787/9789264278547-en>.
- Pagliaro, L., Bouraoui, F., Willems, P., Diels, J., 2014. Large-scale hydrological simulations using the soil water assessment tool, protocol development, and application in the Danube Basin. *J. Environ. Qual.* 43, 145–154. <https://doi.org/10.2134/jeq2011.0359>.
- Palka, E.J., 2005. A Geographic Overview of Panama. In: Harmon, R.S. (Ed.), *The Río Chagres, Panama: A Multidisciplinary Profile of a Tropical Watershed*, Water Science and Technology Library. Springer Netherlands, Dordrecht, pp. 3–18. https://doi.org/10.1007/1-4020-3297-8_1.
- Perez-Valdivia, C., Cade-Menun, B., McMartin, D.W., 2017. Hydrological modeling of the pipestone creek watershed using the Soil Water Assessment Tool (SWAT): Assessing impacts of wetland drainage on hydrology. *J. Hydrol.: Reg. Stud.* 14, 109–129. <https://doi.org/10.1016/j.ejrh.2017.10.004>.
- Qi, J., Zhang, X., Yang, Q., Srinivasan, R., Arnold, J.G., Li, J., Waldhoff, S.T., Cole, J., 2020. SWAT ungauged: water quality modeling in the Upper Mississippi River Basin. *J. Hydrol.* 584, 124601. <https://doi.org/10.1016/j.jhydrol.2020.124601>.
- Roberts, J.T., 2001. Global inequality and climate change. *Soc. Nat. Resour.* 14, 501–509. <https://doi.org/10.1080/08941920118490>.
- Rousta, I., Doostkamian, M., Haghighi, E., Ghafarian Malamiri, H.R., Yarahmadi, P., 2017. Analysis of spatial autocorrelation patterns of heavy and super-heavy rainfall in Iran. *Adv. Atmos. Sci.* 34, 1069–1081. <https://doi.org/10.1007/s00376-017-6227-y>.
- Srinivasan, X., Zhang, J., Arnold, J., 2010. SWAT ungauged: hydrological budget and crop yield predictions in the upper mississippi River Basin. *Trans. ASABE* 53, 1533–1546. <https://doi.org/10.13031/2013.34903>.
- Tan, M.L., Yang, X., 2020. Effect of rainfall station density, distribution and missing values on SWAT outputs in tropical region. *J. Hydrol.* 584, 124660. <https://doi.org/10.1016/j.jhydrol.2020.124660>.
- Tuo, Y., Duan, Z., Disse, M., Chiogna, G., 2016. Evaluation of precipitation input for SWAT modeling in Alpine catchment: a case study in the Adige river basin (Italy). *Sci. Total Environ.* 573, 66–82. <https://doi.org/10.1016/j.scitotenv.2016.08.034>.
- van der Wiel, K., Wanders, N., Selten, F.M., Bierkens, M.F.P., 2019. Added value of large ensemble simulations for assessing extreme river discharge in a 2 °C warmer World. *Geophys. Res. Lett.* 46, 2093–2102. <https://doi.org/10.1029/2019GL081967>.
- Wohl, E., Ogden, F.L., 2013. Organic carbon export in the form of wood during an extreme tropical storm, Upper Río Chagres, Panama. *Earth Surf. Process. Landf.* 38, 1407–1416. <https://doi.org/10.1002/esp.3389>.
- Xu, L., Zheng, C., Ma, Y., 2021. Variations in precipitation extremes in the arid and semi-arid regions of China. *Int. J. Climatol.* 41, 1542–1554. <https://doi.org/10.1002/joc.6884>.
- Xue, F., Shi, P., Qu, S., Wang, J., Zhou, Y., 2018. Evaluating the impact of spatial variability of precipitation on streamflow simulation using a SWAT model. *Water Policy* 21, 178–196. <https://doi.org/10.2166/wp.2018.118>.